J. Biophotonics **7**, No. 6, 425–433 (2014) / **DOI** 10.1002/jbio.201200175

Journal of BIOPHOTONICS

FULL ARTICLE

Real-time interactive two-photon photoconversion of recirculating lymphocytes for discontinuous cell tracking in live adult mice

Tatyana Chtanova[*,**,1,2], *Henry R. Hampton*[1,2], *Louise A. Waterhouse*[1], *Katherine Wood*[1], *Michio Tomura*[3], *Yoshihiro Miwa*[4], *Charles R. Mackay*[5], *Robert Brink*[1,2], *and Tri Giang Phan*[*,**,1,2]

[1] Immunological Diseases Division, Garvan Institute of Medical Research, Sydney, Australia
[2] St Vincent's Clinical School, Faculty of Medicine, University of New South Wales, Sydney, Australia
[3] Center for Innovation in Immunoregulative Technology and Therapeutics, Kyoto University Graduate School of Medicine, Kyoto, Japan
[4] Department of Molecular Pharmacology, Graduate School of Comprehensive Human Sciences, University of Tsukuba, Tsukuba, Japan
[5] Immunology Department, Monash University, Melbourne, Australia

Received 3 September 2012, revised 15 October 2012, accepted 21 October 2012
Published online 27 November 2012

Key words: multiphoton fluorescence microscopy, optics and photonics, Kaede protein, cell tracking

Supporting information for this article is available free of charge under http://dx.doi.org/10.1002/jbio.201200175

The potential usefulness of intravital two-photon microscopy for fate mapping is limited by its inability to track cells beyond the confines of the imaging volume. Therefore, we have developed and validated a novel method for in vivo photolabelling of spatially-restricted cells expressing the Kaede optical highlighter by two-photon excitation. This has allowed us to optically mark a cohort of follicular B cells and track their dissemination from the original imaging volume in the lymph node to the spleen and contralateral lymph node. We also present the first demonstration, to our knowledge, of in vivo photoconversion of a freely moving single cell in a live adult animal. This method of 'discontinuous' cell tracking therefore significantly extends the fate mapping capabilities of two-photon microscopy to delineate the spatiotemporal dynamics of cellular processes that span multiple anatomical sites at the single cell level.

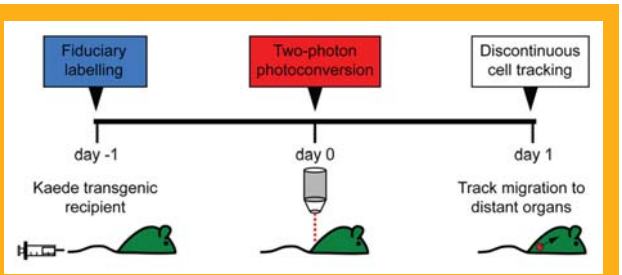

Intravital two-photon photoconversion enables targeted optical marking of Kaede cells in precise microanatomical compartments and their discontinuous tracking to distant anatomical sites over a period of days to weeks.

1. Introduction

Lymphocytes recirculate between the blood, lymph and lymphatic tissues to continuously monitor for threats from infectious pathogens [1]. Pathogens that have breached surface defenses are trapped in the draining lymph node where they rapidly activate antigen-specific lymphocytes. Multiple effector and mem-

* Corresponding authors: e-mail: t.chtanova@garvan.org.au or t.phan@garvan.org.au, Phone: +61 2 92958414 or +61 2 92958404, Fax: +61 2 92958404
** These authors contributed equally to this work.

ory cells are then generated which are deployed via the blood to the original inflammatory foci and other lymphatic tissues. Thus, comprehensive analysis of the dynamics of the immune response requires the ability to longitudinally track cells from the initial stages of cellular activation in the lymph node to their deployment to the periphery over a period of days to weeks.

Optical highlighters are molecules that can be photoactivated (turned from off to on), photoswitched (turned on and off repeatedly) or photoconverted (spectrally shifted from one wavelength to another) by irradiation with light [2]. Genetically encoded optical highlighters have been extensively used to label and track the trafficking of proteins and organelles within cells, and the migration of cells within small imaging volumes [3]. Kaede is a fluorescent coral protein that undergoes a spectral shift in its peak emission from 518 nm (green) to 582 nm (red) upon exposure to UV or violet light [4]. Transgenic mice expressing Kaede have been used to non-specifically label and track the migration of immune cells in lymph nodes [5] and skin [6]. While these studies highlighted the potential for cell tracking using Kaede, the non-targeted irradiation of exposed tissue lacks the spatial resolution required to distinguish cells located at different depths and within different microanatomical compartments. Furthermore, irradiation with UV light is phototoxic [5, 6].

Two-photon excitation (TPE) microscopy is the gold-standard for deep tissue imaging under near physiological conditions [7, 8] and has transformed fields of research such as immunology [9, 10]. The use of high repetition rate ultrafast near infra-red (NIR) laser light offers several advantages including confinement of the excitation volume to the focal plane and negligible phototoxicity and photobleaching [11]. The power of TPE was demonstrated by its recent application to precisely bulk label cells expressing PA-GFP within the germinal center of live mice [12]. One drawback of the PA-GFP approach, however, is that target cells are not easily visible prior to photoactivation. This makes it difficult to adjust the laser power intensity or duration to avoid phototoxicity during photoconversion.

Here we have used a conventional turnkey two-photon microscope to photoconvert Kaede transgenic cells in intact lymph nodes of live mice without perturbing cell viability, motility or trafficking properties. This method can be used to label large regions of interest (ROIs) within specific areas of the lymph node as well as to target single cells of interest. Moreover, intravital two-photon photoconversion (TPP) offers the advantage that optically marked cells can be tracked to distant organs when combined with recovery surgery. The power of this approach is demonstrated by the specific labelling of follicular B cells in the lymph node to directly examine their recirculation kinetics as they traffic between spatially separated lymphoid organs. These data show that optical highlighting by TPP is a powerful new tool for long-term "discontinuous" cell tracking and fate mapping across multiple anatomical compartments in live animals.

2. Experimental

2.1 Mice and adoptive cell transfers

Kaede transgenic mice [5] were backcrossed and maintained on C57BL/6 background. C57BL/6 mice were from the Animal Resources Centre (Canning Vale, WA) and Australian BioResources (Moss Vale, NSW). Albino C57BL/6 mice with spontaneous mutations in the tyrosinase gene (000058; B6(Cg)-*Tyr*$^{c-2J}$/J) [13] and C57BL/6 mice expressing CFP under the β-actin promoter (004218; Tg(ACTB-ECFP) [14] were from Jackson Laboratories. Mice were housed in specific-pathogen free conditions. The Garvan Institute of Medical Research/St Vincent's Hospital Animal Ethics Committee approved all animal experiments.

B cells were isolated from spleens of Kaede and CFP transgenic mice by AutoMACS (Miltenyi) negative selection using biotinylated antibodies against CD11c and CD43 (BD Pharmingen) and MACS anti-biotin microbeads (Miltenyi) [15]. Cells were >97% pure as assessed by FACS staining for B220-APC clone RA3-6B2 (BD Pharmingen). Typically, 10^7 purified B cells were then adoptively transferred into wild-type recipient mice 1–3 days before two-photon microscopy. Recipient mice also received CFP B cells and were injected subcutaneously with anti-CD157-Alexa Fluor647 clone BP3 (UCSF Hybridoma Core) to label the B cell follicle [16].

For FACS analysis, single cell suspensions were stained with B220-Pacific Blue clone RA3-6B2, CD4-PerCp clone RM4-5 and DAPI (Invitrogen) to determine the green and red fluorescence of unphotoconverted and photoconverted Kaede cells. Multiparameter data was acquired on a 7-laser LSRII SORP high-speed analyser (BD Biosciences) and analysed using FlowJo software (Tree Star Inc.).

2.2 Two-photon microscopy

We used an upright Zeiss 7MP two-photon microscope (Carl Zeiss) with a W Plan-Apochromat 20×/1.0 DIC (UV) Vis-IR water immersion objective. For spectral fingerprints we used an LBF 690 short pass IR blocking filter and BSMP 690 dichroic for the non-descanned detector (NDD) sideport. For other experiments we used a LBF 760 and BSMP

760 to enable detection of the far-red emission of Alexa Fluor647. Four external NDDs were used to detect blue (SP 485), green (BP 500–550), red (BP 565–610) and far-red (BP 640–710). High repetition rate femtosecond pulsed NIR excitation was provided by a Chameleon Vision II Ti : Sa laser (Coherent Scientific). Explanted lymph nodes were perfused with warm RPMI diffused with 5% CO_2/95% O_2 as described [16]. We acquired 512 × 512 pixel images with dwell time of 1.27 µs/pixel at 2–3 µm z-step intervals using bidirectional scanning. Time-lapse images were acquired at 30 s intervals.

Intravital two-photon microscopy was based on a previously described method [15]. Mice were induced with 100 mg/kg ketamine/5 mg/kg xylazine and maintained with 1–2% isoflurane supplemented with 100% oxygen at a flow rate of 500 ml/min via a nose cone. Anesthetised mice were kept warm using a customised heated SmartStage (Biotherm). The skin was shaved and a flap containing the inguinal ligament and lymph node was immobilised on a base of thermal conductive T-putty (Thermagon Inc.) by gluing the edges with Vetbond tissue adhesive (3M) to isolate it from respiratory and cardiac movements. A small window was made in the skin and fascia and fat microdissected using low-level illumination with a Stemi stereomicroscope (Zeiss) to expose the lymph node. For recovery surgery, we sutured the skin and carefully closed the skin flap with Vetbond. Mice were given opiate analgesia (buprenorphine 0.075 mg/kg given subcutaneously) post-operatively and allowed to mobilise freely for 24 hours before they were sacrificed.

2.3 TPE and TPP fingerprinting

The Ti : Sa laser output at the objective was measured with a Fieldmaster portable power meter (Coherent Scientific) and a laser power calibration curve generated for λ scanning. Excitation lambda stacks were then acquired using the Excitation Fingerprint macro in the ZEN software (Carl Zeiss). Measured fluorescence intensity was then normalised to the peak fluorescence. TPP was performed by bidirectional scanning with 840 nm NIR laser pulses. We scaled the laser power intensity and duration of the irradiation from 20–60 mW and 500–5,000 cycles, respectively, depending on the size of the ROI.

2.4 Image processing and data analysis

Mean pixel fluorescence intensities were extracted using the Mean of ROI function in ZEN software and exported to Microsoft Excel. Background signal was subtracted and the adjusted and normalised fluorescence calculated before graphical analysis in GraphPad Prism (GraphPad Software). Raw image files were processed using Imaris Bitplane Software. A Gaussian filter was applied to reduce background noise. Tracking was performed using Imaris spot detection function to locate the centroid of cells. Motility parameters such as track length (calculated as the total length of displacements within the track) and track speed (calculated by dividing track length by time) were obtained using Imaris Statistics function. Maximum intensity projection time-lapse images were exported and videos were compiled and annotated using Adobe AfterEffects. Movies were compressed using MacX Video Converter Pro (Digiarty Software).

All modelling and statistical analysis was performed in GraphPad Prism. Non-linear regression analysis of photoconversion showed it best fitted a first-order polynomial model. Similar analysis of photobleaching showed it best fitted a two-phase exponential decay model. Linear regression was performed to determine the relationship between log-fluorescence intensity and log-laser power, and the relationship between fluorescence intensity and photoconversion depth. Means between two normally distributed groups were compared using a Student's t-test.

3. Results and discussion

3.1 Detection of Kaede in deep tissue by TPE

To determine the TPE spectra and optimal wavelengths for detecting unphotoconverted ("green") and photoconverted ("red") Kaede we irradiated lymph nodes from Kaede transgenic mice [5] ex vivo with violet light for 30 minutes. Photoconversion was associated with >4,000-fold increase in red fluorescence in $B220^+$ B cells and >2,000-fold increase in $CD4^+$ T cells, respectively, with a corresponding 80–90% decrease in green fluorescence (Figures 1a and S1). Irreversibly marked cells could be detected >7 days later (Ref. [5] and Figure S1). Lymph nodes were then λ-scanned from 700 to 1040 nm before and after photoconversion to obtain a TPE profile for the green and red Kaede protein (Figures 1b, c and S2, S3). We also detected fluorescence signal from the photoconverted lymph node between 890 and 1030 nm due to spectral bleed-through from residual unphotoconverted Kaede protein (Ref. [5], Figures 1a, c and S4). Thus, photoconverted Kaede can be optimally excited at 770 nm and readily discriminated from unphotoconverted Kaede for deep tissue imaging by TPE.

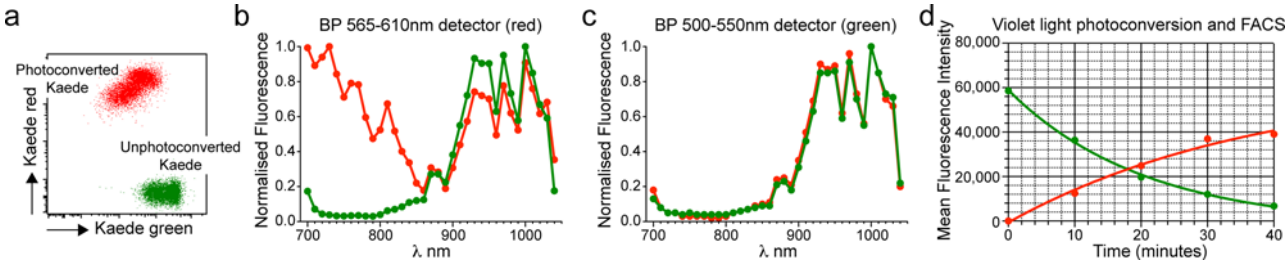

Figure 1 Characterization of Kaede TPE spectra (**a**) Photoconverted lymph nodes (red dots) from Kaede transgenic mice were analyzed by FACS together with non-photoconverted lymph nodes (green dots). (**b**, **c**) TPE spectral profiles for photoconverted (red) and non-photoconverted (green) Kaede. (**d**) Kaede transgenic lymph nodes were exposed to violet light for varying time intervals and the Mean Fluorescence Intensities (MFI) analyzed by FACS.

3.2 Photoconversion of Kaede in deep tissue by TPE

We next set out to determine whether we can achieve efficient photoconversion in intact lymph nodes by TPE. To identify the optimum TPP wavelength we created a photoconversion profile by scanning equivalent $10.6 \times 10.6\,\mu m$ ROIs from 740–880 nm in 20 nm steps in relatively flat areas of the lymph node beneath the cortical surface (Figure 2a). The lymph node was then scanned at 770 nm and the photoconverted ROIs analyzed for red fluorescence to obtain a TPP spectral fingerprint (Figure 2b). These data showed photoconversion peaks at 800 and 840 nm (Figure 2b). Kinetic analysis showed that the TPP was fastest for the shorter wavelengths (Figure 2c). To measure the corresponding photobleaching rates, $10.6 \times 10.6\,\mu m$ ROIs from maximally photoconverted Kaede transgenic lymph nodes were scanned at 740, 800, 840 and 860 nm at the same depth and laser power. This showed that photobleaching fitted a two-phase decay model with faster decay rates and lower plateaus for 740 and 800 nm compared to 840 and 860 nm (Figure 2d). Thus, the faster photoconversion at 740 nm versus 840 nm is offset by more rapid and extensive photobleaching. Furthermore, as expected, the TPP effi-

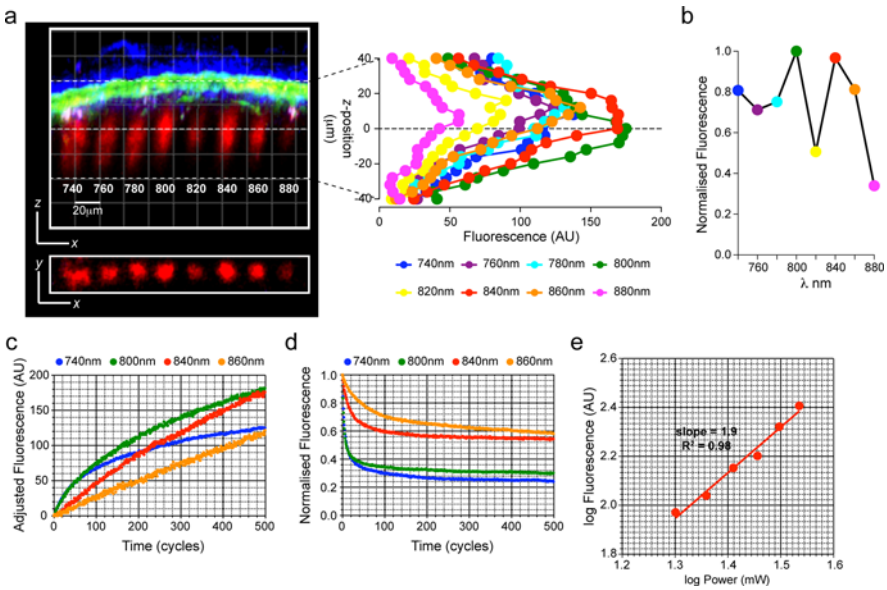

Figure 2 Characterization of Kaede TPP spectra. (**a**) TPP profile generated by irradiating a ROI with NIR laser from 740 to 880 nm and imaging at 770 nm. Photoconverted Kaede (red), non-photoconverted Kaede (green), SHG (blue), autofluorescent macrophages (pink). Top panel zx projection of a 3D volume. Bottom panel, single xy slice in the photoconversion plane. Right panel shows quantification of red fluorescence against z-position for the different photoconversion wavelengths. (**b**) Normalized red fluorescence from (**a**) was plotted against photoconversion wavelengths. (**c**) Photoconversion rates for different wavelengths. (**d**) Photobleaching rates for different wavelengths. (**e**) Log-log plot of laser power against photoconverted red fluorescence signal. Data is representative of at least three independent experiments.

ciency of the shorter 740 nm wavelength dropped off much more steeply at increasing depths compared to 840 nm (Figure S5). Finally, we measured the dependence of the TPP signal on the laser power intensity (Figure 2e). The log–log plot of this revealed a slope of 1.9 ± 0.2 indicating that the photoconversion had a quadratic dependence on laser power, as predicted for a TPE process [11]. Thus, by taking into account both photoconversion and photobleaching rates and light scattering factors, we concluded that Kaede is optimally photoconverted by TPE at 840 nm in opaque tissues.

3.3 Microanatomical labelling with Kaede

To assess the point spread function (PSF) of TPP, we photoconverted 85×85 μm ROIs in explanted lymph nodes which were maintained at room temperature to minimize any cellular movement that might affect the photoconversion efficiency and spatial confinement (Figure 3a). Analysis of the photoconverted red fluorescence signal showed that the axial full-width half-maximum (FWHM) under these conditions was 17 μm (Figure 3b). Furthermore, by adjusting the size of the ROI, laser power intensity and duration, pixel density and pixel dwell time we could expand the photoconversion volume in the axial plane (for example, from $85 \times 85 \times 20$ to $85 \times 85 \times 60$ μm) with minimal photobleaching. To demonstrate specific photolabelling of a spatially-restricted cell type, we targeted six large ROIs (containing 6,000–12,000 cells in total) in the B cell follicle identified by the presence CFP B cells, and analysed the phenotype of the photoconverted cells by FACS (Figure 3c). This showed that >97% of the photoconverted cells were B220$^+$ B cells (Figure 3c). Thus, we can precisely photolabel cells based on their microanatomical location. We also showed that

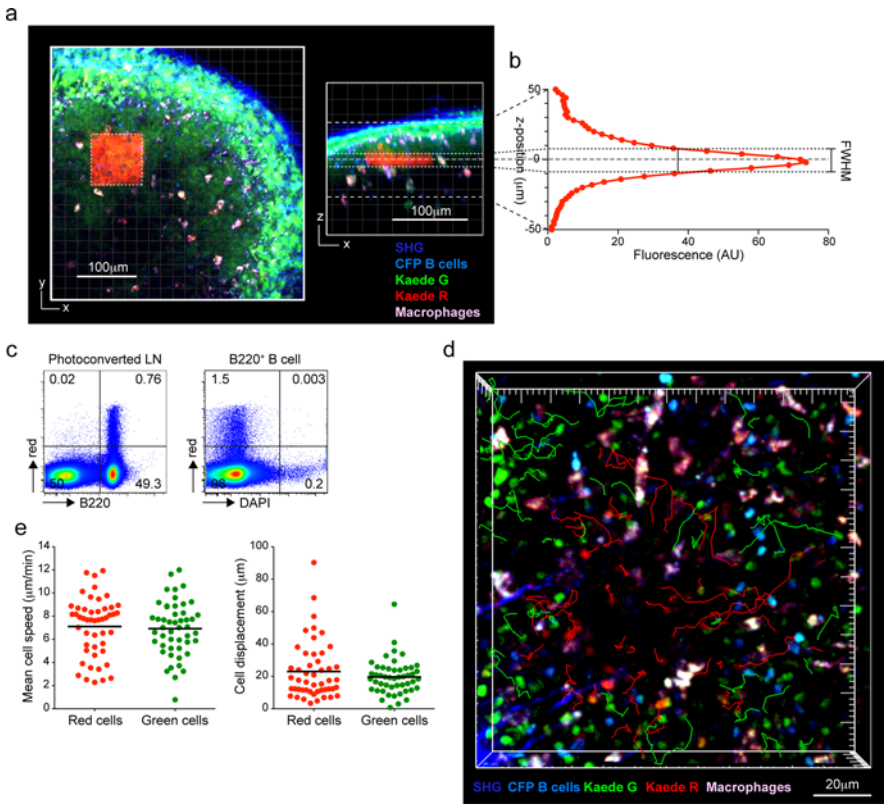

Figure 3 Microanatomical labelling by Kaede TPP. (**a**) ROIs were photoconverted by irradiation with 840 nm laser pulses. Photoconverted Kaede (red), unphotoconverted Kaede (green), SHG (blue), autofluorescent macrophages (pink). Left panel shows a projection in *xy*, right panel projection in *xz*, acquired at 770 nm. (**b**) FWHM was determined by plotting fluorescence intensity against *z*-position. (**c**) FACS analysis of photoconverted lymph nodes shows specific labelling of spatially-restricted B220$^+$ B cells (left panel) and DAPI exclusion by photoconverted cells (right panel). (**d**) Still-frame of a time-lapse series taken at 810 nm in a perfused inguinal lymph node immediately after photoconversion. Selected tracks (red – photoconverted Kaede B cells, green – non-photoconverted Kaede B cells) are shown. CFP transgenic B cells (cyan) were co-transferred to mark the B cells follicles. Corresponds to Video S1. (**e**) Quantification of cell speed and displacement of photoconverted (red) and non-photoconverted (green) Kaede transgenic B cells. Data are representative of at least three independent experiments.

cell viability was not affected by photoconversion as assessed by DAPI staining (Figure 3c). To determine their motility, we photoconverted adoptively transferred Kaede B cells at depths of 80–100 μm below the capsule. Time-lapse images captured immediately after photoconversion showed that photoconverted B cells migrated with comparable mean velocities and displacements as non-photoconverted B cells in equivalent volumes of the follicle (Figure 3d, e and Video S1). Thus, localised photoconversion can label cells within microanatomical compartments with no impact on cell viability or motility.

3.4 Discontinuous cell tracking with Kaede

We next asked if photoconverted cells were able to traffick normally to other lymphoid tissue under homeostatic conditions (Figure 4a). CFP B cells were adoptively transferred to label the follicle and we photoconverted six ROIs containing 6–12,000 cells (Figure 4b). Intravital TPP was associated with significant migration of the photoconverted cells outside the ROI by the end of irradiation (Figure 4c). FACS analysis 24 hours after recovery from anesthesia showed that only ~100 of the estimated 6,000 photoconverted Kaede B cells remained in the photoconverted lymph node (Figure 4d). We detected ~100 photoconverted Kaede B cells in the contralateral inguinal lymph node and ~2,000 cells in the spleen. In contrast, red Kaede B cells could not be detected in the lymph nodes or spleen of sham-photoconverted mice (Figure 4d). This is consistent with a lymph node dwell time of <24 hours.

3.5 In vivo photoconversion of freely moving single cells

Localised TPP also makes it possible to photoconvert single cells of interest instead of bulk populations. A major obstacle to in vivo single cell photoconversion, however, is the fact that lymphocytes are highly motile cells under physiological conditions (Figure 3d, e and Video S1). This became apparent during photoconversion of ROIs when Kaede green cells were observed to migrate in and out of the photoconversion volume (Figure S6 and Video S2). Therefore, we took advantage of the fact that Kaede cells can be visualised before photoconversion by their green fluorescence at 840 nm (but not at 800 nm; Figure 1b) to continuously track and main-

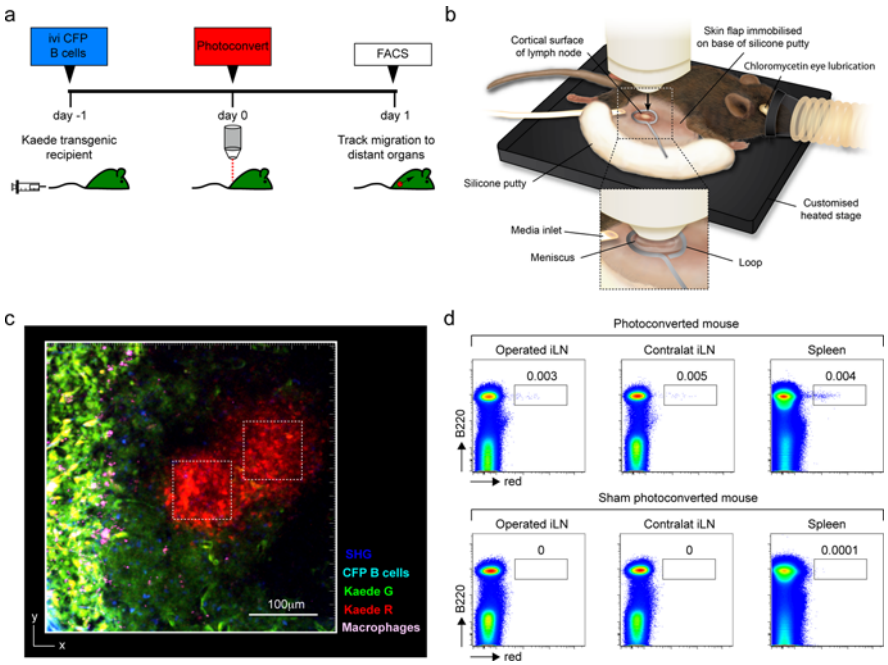

Figure 4 Intravital TPP and cell fate mapping. (**a**) Experimental setup for discontinuous cell tracking. (**b**) Method for imaging and recovery surgery. (**c**) Kaede red cells migrate out from the ROI immediately after photoconversion. Still-frame projection of a 3D volume imaged at 810 nm immediately after photoconversion of two ROIs. Photoconverted Kaede (red), unphotoconverted Kaede (green), CFP B cells (cyan), SHG (blue), macrophages (pink). (**d**) FACS analysis of photoconverted lymph node, contralateral lymph nodes and spleen 24 hours later from photoconverted (top panel) and sham-photoconverted control mouse (bottom panel). Data are representative of at least two independent experiments.

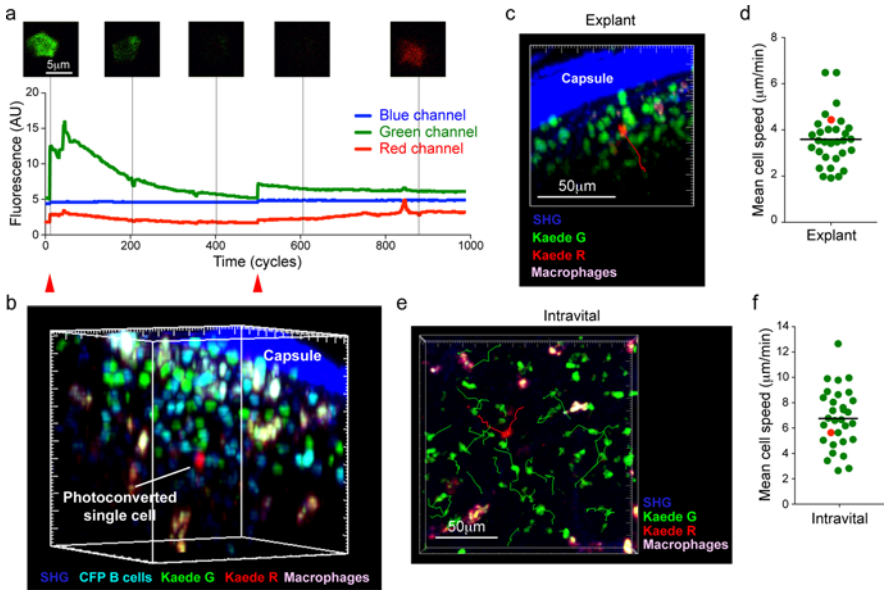

Figure 5 In vivo single cell photoconversion (**a**) Real-time interactive tracking and single cell photoconversion. Arrowheads indicate the time-points when the laser power was adjusted. Representative still-frames from a time-lapse real-time photoconversion series are shown. Corresponds to Video S3. (**b**) Single cell photoconversion. 3D reconstruction taken immediately after photoconversion imaged at 810 nm and 920 nm. A photoconverted Kaede B cell (red) is surrounded by non-photoconverted Kaede B cells (green) and CFP B cells (cyan), SHG (blue). (**c**) Still-frame from a time-lapse series imaged at 810 nm in a perfused inguinal lymph node immediately after photoconversion. Photoconverted Kaede (red), non-photoconverted Kaede (green), SHG (blue), autofluorescent macrophages (pink). The path of the photoconverted lymphocyte is shown in red. Corresponds to Video S4. (**d**) Mean cell speed for photoconverted (red) and non-photoconverted (green) Kaede cells from (**c**). (**e**) Projection of a time-lapse series imaged at 810 nm in an inguinal lymph node immediately after photoconversion in a live animal. Photoconverted Kaede (red), non-photoconverted Kaede (green), SHG (blue), autofluorescent macrophages (pink). The path of the photoconverted lymphocyte is shown in red. Corresponds to Video S5. (**f**) Mean cell speed for photoconverted (red) and non-photoconverted (green) Kaede cells from (**e**).

tain the cell inside the desired ROI using the real-time interactive display (Figure 5a). For this, we adoptively transferred Kaede transgenic B cells together with CFP B cells into wild-type recipient mice and scaled the ROI down to a single cell volume. Initially, targeted cells displayed green and red fluorescence (from spectral bleed-through of the Kaede green). As the cell was irradiated, there was a gradual loss of green and red signals followed by acquisition of red fluorescence from photoconverted Kaede red (Figure 5a and Video S3). Thus we could fine-tune the laser power intensity and duration in response to real-time read-outs of the fluorescence signal. Dual wavelength scanning at 810 nm (to detect Kaede red at depth with minimal photobleaching) and 920 nm (to detect Kaede green) at the end of the photoconversion cycles confirmed successful single cell photoconversion without any off-target photoconversion of neighbouring cells (Figure 5b). Importantly, photoconverted single cells maintained normal motility during and immediately after the photoconversion. For example, in one explant preparation, the photoconverted single cell was observed to migrate from the subcapsular region into the deeper follicle (Figure 5c and Video S4) with comparable motility to non-photoconverted cells (Figure 5d and Video S4). Finally, we applied the method to intravital microscopy where tissue movement from respiration and cardiac pulsations can pose additional challenges to maintaining a stable imaging platform. By immobilising the inguinal lymph node using the intravital skin flap preparation we were able to precisely photoconvert single cells (Figure 5e) without any perturbation to cell motility (Figure 5f and Video S5). To our knowledge, this is the first demonstration of in vivo photomanipulation of a single motile cell in a live adult mouse.

4. Conclusion

In this study we describe a novel method for localised photoconversion in deep tissue of live animals that can be scaled from large ROIs to the single cell level. Our method allows the laser power intensity and duration to be adjusted in response to the fluorescence signal in real-time to maximise photocon-

version and minimise phototoxicity and photobleaching. When combined with survival surgery and down-stream analysis by high speed FACS and ancillary techniques, intravital two-photon photoconversion of Kaede is a powerful technique that can be used for microanatomical labelling and tracking of cell migration over large distances and time scales within whole animals that is beyond the scope of current microscopic techniques. The method is therefore ideally suited to the study of hemopoietic and immune systems where cells constantly recirculate via the blood and lymph.

Here, we have characterised the TPE spectral fingerprints of Kaede in biological specimens where large autofluorescent cells (such as macrophages) and stromal elements (such as blood vessels) can degrade image quality due to microlensing and light scattering effects [8]. Our analysis of the TPP 'fingerprint', photobleaching and photoconversion rates enabled us to determine 840 nm was the optimal photoconversion wavelength. Furthermore, unphotoconverted Kaede green is more visible at 840 nm than 800 nm allowing us to continuously track and photoconvert the target cell as it migrated within the lymph node in real-time without the need for a dual scanning system with two NIR lasers. We were also able to achieve a high level of precision in the three-dimensional targeting of photoconversion. Since cytoplasmic Kaede is free to diffuse within photoconverted cells, the measured axial point spread of 16–18 μm compares favorably with the predicted FWHM of 16 μm (for a cell diameter of 8–10 μm) given that some of the photoconverted cells will lie above and below the photoconversion plane.

Importantly, our method for intravital microscopy and recovery surgery realizes the potential of irreversible optical highlighters such as Kaede for 'discontinuous' tracking of cell fates over extended time intervals. In this method, photoconverted cells that have left the imaging volume can be tracked to distal sites long after mice have recovered from anesthesia. The ability of photoconverted B cells to equilibrate across the entire B cell compartment after 24 hours indicates that our microsurgery did not damage any lymphatic or blood vessels nor did it cause any lymph node 'shutdown' [17]. Our data agrees with previous studies of lymphocyte recirculation that have provided estimates of the average lymph node residence time of 12–24 hours [18–20]. We have combined localised photoconversion with recovery surgery to examine the kinetics of follicular B cell recirculation as proof-of-concept. Future studies will use these techniques to examine the kinetics of lymphocyte recirculation in homeostasis and track the fate of effector and memory cells in an ongoing immune response.

TPP of Kaede has been previously performed in turbid media [21] and in vitro cell cultures under non-physiological conditions [22]. Other investigators have successfully photolabelled single non-motile neurons in optically transparent zebrafish embryos [23]. However, ours is the first report to show the precise targeting, labelling and tracking of motile single cells within a living adult mammal. Our demonstration paves the way for other applications that require the precise delivery of light of defined energies and wavelengths to "switch" on or off biological processes in a moving target cell. In this instance we have used Kaede but our strategy can be applied to the growing list of optical highlighters such as Kikume [24] and dendra [25]. While we have initially applied our method to answer immunological questions, we expect our method could be applied to track the migration and fate of any number of cells of interest from one tissue to another over a period of days to weeks.

Acknowledgments We thank A. Bullen for discussions and E. Robey, A. Basten, S. Tangye and D. Suan for comments on the manuscript. Supported by Peter and Val Duncan, Human Frontiers Science Program, Cancer Institute NSW, National Health and Medical Research Council (1004632), NHMRC Career Development Fellowships (T.C. and T.G.P.) and Australian Postgraduate Award (H. H.).

Author biographies Please see Supporting Information online.

References

[1] E. C. Butcher and L. J. Picker, Science **272**(5258), 60–66 (1996).
[2] G. H. Patterson, J Microsc **243**(1), 1–7 (2011).
[3] K. A. Lukyanov, Nat Rev Mol Cell Biol **6**(11), 885–891 (2005).
[4] R. Ando, H. Hama, M. Yamamoto-Hino, H. Mizuno, and A. Miyawaki, Proc Natl Acad Sci USA **99**(20), 12651–12656 (2002).
[5] M. Tomura, N. Yoshida, J. Tanaka, S. Karasawa, Y. Miwa, A. Miyawaki, and O. Kanagawa, Proc Natl Acad Sci USA **105**(31), 10871–10876 (2008).
[6] M. Tomura, T. Honda, H. Tanizaki, A. Otsuka, G. Egawa, Y. Tokura, H. Waldmann, S. Hori, J. G. Cyster, T. Watanabe, Y. Miyachi, O. Kanagawa, and K. Kabashima, J Clin Invest **120**(3), 883–893 (2010).
[7] W. Denk, J. H. Strickler, and W. W. Webb, Science **248**(4951), 73–76 (1990).
[8] F. Helmchen and W. Denk, Nat Methods **2**(12), 932–940 (2005).
[9] M. D. Cahalan and I. Parker, Annu Rev Immunol **26**, 585–626 (2008).
[10] T. G. Phan and A. Bullen, Immunol Cell Biol **88**(4), 438–444 (2010).
[11] W. R. Zipfel, R. M. Williams, and W. W. Webb, Nat Biotechnol **21**(11), 1369–1377 (2003).

[12] G. D. Victora, T. A. Schwickert, D. R. Fooksman, A. O. Kamphorst, M. Meyer-Hermann, M. L. Dustin, and M. C. Nussenzweig, Cell **143**(4), 592–605 (2010).
[13] D. Townsend, C. J. Witkop, Jr., and J. Mattson, J Exp Zool **216**(1), 113–119 (1981).
[14] A. K. Hadjantonakis, S. Macmaster, and A. Nagy, BMC Biotechnol **2**, 11 (2002).
[15] T. G. Phan, I. Grigorova, T. Okada, and J. G. Cyster, Nat Immunol **8**(9), 992–1000 (2007).
[16] T. G. Phan, J. A. Green, E. E. Gray, Y. Xu, and J. G. Cyster, Nat Immunol **10**(7), 786–793 (2009).
[17] I. McConnell, J. Hopkins, and P. Lachmann, Ciba Found Symp **71**, 167–195 (1980).
[18] W. L. Ford and S. J. Simmonds, Cell Tissue Kinet **5**(2), 175–189 (1972).
[19] J. Westermann, Z. Puskas, and R. Pabst, Scand J Immunol **28**(2), 203–210 (1988).
[20] I. L. Grigorova, M. Panteleev, and J. G. Cyster, Proc Natl Acad Sci USA **107**(47), 20447–20452 (2010).
[21] K. Isobe, H. Hashimoto, A. Suda, F. Kannari, H. Kawano, H. Mizuno, A. Miyawaki, and K. Midorikawa, Biomed Opt Express **1**(2), 687–693 (2011).
[22] W. Watanabe, T. Shimada, S. Matsunaga, D. Kurihara, K. Fukui, and S. Shin-Ichi Arimura, Opt Express **15**(5), 2490–2498 (2007).
[23] K. Hatta, H. Tsujii, and T. Omura, Nat Protoc **1**(2), 960–967 (2006).
[24] H. Tsutsui, S. Karasawa, H. Shimizu, N. Nukina, and A. Miyawaki, EMBO Rep **6**(3), 233–238 (2005).
[25] N. G. Gurskaya, V. V. Verkhusha, A. S. Shcheglove, D. B. Staroverov, T. V. Chepurnukh, A. F. Fradkov, S. Lukyanov, and K. A. Lukyanov, Nat Biotechnol **24**(4), 461–465 (2006).